X-ray magnetic circular dichroism for Co x Fe4 − x N (x = 0, 3, 4) films grown by molecular beam epitaxy

著者	Ito Keita, Sanai Tatsunori, Yasutomi Yoko, Zhu Siyuan, Toko Kaoru, Takeda Yukiharu, Saitoh Yuji, Kimura Akio, Suemasu Takashi
journal or publication title	Journal of applied physics
volume	115
number	17
page range	17C712
year	2014-05
権利	(C) 2014 AIP Publishing LLC This article may be downloaded for personal use only. Any other use requires prior permission of the author and the American Institute of Physics. The following article appeared in J. Appl. Phys. 115, 17C712 (2014) and may be found at http://dx.doi.org/10.1063/1.4862517.
URL	http://hdl.handle.net/2241/00121611

doi: 10.1063/1.4862517

X-ray magnetic circular dichroism for Co x Fe4 x N (x=0, 3, 4) films grown by molecular beam epitaxy

Keita Ito, Tatsunori Sanai, Yoko Yasutomi, Siyuan Zhu, Kaoru Toko, Yukiharu Takeda, Yuji Saitoh, Akio Kimura, and Takashi Suemasu

Citation: Journal of Applied Physics **115**, 17C712 (2014); doi: 10.1063/1.4862517
View online: http://dx.doi.org/10.1063/1.4862517
View Table of Contents: http://scitation.aip.org/content/aip/journal/jap/115/17?ver=pdfcov
Published by the AIP Publishing

X-ray magnetic circular dichroism for $Co_xFe_{4-x}N$ ($x = 0, 3, 4$) films grown by molecular beam epitaxy

Keita Ito,[1] Tatsunori Sanai,[1] Yoko Yasutomi,[1] Siyuan Zhu,[2] Kaoru Toko,[1] Yukiharu Takeda,[3] Yuji Saitoh,[3] Akio Kimura,[2] and Takashi Suemasu[1,a)]
[1]*Institute of Applied Physics, Graduate School of Pure and Applied Sciences, University of Tsukuba, 1-1-1 Tennodai, Tsukuba, Ibaraki 305-8573, Japan*
[2]*Graduate School of Science, Hiroshima University, 1-3-1 Kagamiyama, Higashi-Hiroshima, Hiroshima 739-8526, Japan*
[3]*Condensed Matter Science Division, Japan Atomic Energy Agency, 1-1-1 Kouto, Sayo-cho, Hyogo 679-5148, Japan*

(Presented 5 November 2013; received 20 September 2013; accepted 22 October 2013; published online 27 January 2014)

We evaluated orbital (m_{orb}) and spin magnetic moments (m_{spin}) of $Co_xFe_{4-x}N$ ($x = 0$, 3, 4) epitaxial thin films grown by molecular beam epitaxy using x-ray magnetic circular dichroism, and discussed the dependence of these values on x. Site-averaged m_{spin} value of Fe atoms was deduced to be 1.91 μ_B per atom, and that of Co atoms to be 1.47 μ_B per atom in Co_3FeN at 300 K. These values are close to 1.87 μ_B per Fe atom in Fe_4N and 1.43 μ_B per Co atom in Co_4N, respectively. This result implies that the Fe and Co atoms in the Co_3FeN films were located both at corner and face-centered sites in the anti-perovskite lattice. Spin magnetic moments per unit cell were decreased linearly with increasing x in $Co_xFe_{4-x}N$. This tendency is in good agreement with theory predicted by the first-principle calculation. © *2014 AIP Publishing LLC*. [http://dx.doi.org/10.1063/1.4862517]

I. INTRODUCTION

Ferromagnetic nitrides are composed of abundant non-toxic elements. Synthesis of bulk and thin films, and characterization of their physical properties were promoted for application to magnetic recording media and spintronics devices. Figure 1 shows the lattice structure of anti-perovskite type ferromagnetic nitrides, which is constructed by a fcc lattice of 3*d* transition atoms and a body-centered nitrogen atom. The corner (I) and face-centered (II) atomic sites of the cubic lattice become non-equivalent due to the existence of nitrogen atoms. In addition, II sites can be separated into IIA and IIB sites by considering hybridization of electron orbits between 3*d* atoms and N atoms. Among them, the spin-polarization of density of states (P) at the Fermi level (E_F) was calculated to be −0.60 in Fe_4N, and the spin-polarization of electrical conductivity (β) to be −1.0.[1] Large negative P was also predicted in Co_4N (−0.88 at E_F)[2] and in Co_3FeN (−0.75 at E_F), where Fe atoms at the II sites of Fe_4N are replaced by Co atoms.[3] We therefore consider $Co_xFe_{4-x}N$ promising for application to spintronics devices. We have already evaluated β of Fe_4N films grown by molecular beam epitaxy (MBE) on MgO(001) substrates using point contact Andreev reflection, and shown that Fe_4N has larger $|\beta|$ than α-Fe.[4] In the CoFeB/MgO/Fe_4N magnetic tunnel junctions formed by sputtering method, inverse tunnel magnetoresistance effect of −75% was reported at room temperature.[5] We have achieved the epitaxial growth of $Co_xFe_{4-x}N$ ($x = 0$, 3, 4) thin films by means of MBE on $SrTiO_3$(STO)(001) substarates,[6–8] and characterized orbital (m_{orb}) and spin magnetic moments (m_{spin}) of MBE-grown Fe_4N[9] and Co_4N[10] films using x-ray magnetic circular dichroism (XMCD) measurements. However, there have been no reports on the element specific magnetic moments of Co_3FeN. In this study, we performed XMCD measurements for MBE-grown Co_3FeN films and deduced their element specific m_{orb} and m_{spin}. In addition, m_{orb} and m_{spin} in Fe_4N and Co_4N were revalued by a more precise analysis method for obtained XMCD spectra. Although Co_4N has larger $|P|$ than Co_3FeN, we think that Co_3FeN is more suitable for application to spintronics devices. This is because the body-centered N atoms in Co_4N tend to be deficient, probably making its $|P|$ smaller than expected. In our previous work about x-ray diffraction measurements on Co_4N and Co_3FeN films,[7,8] the peak intensity of Co_4N(001) was much smaller than that of Co_3FeN(001). According to the x-ray extinction rule, the diffraction peak of Co_4N(001) is present when the N atoms are located at the body center of the cube. But the (001) diffraction is forbidden when the N atoms are absent. These results show that the N atoms in Co_4N became deficient. For applications of Co_3FeN spintronics devices, characterization of basic physical properties of Co_3FeN is a requirement. Other anti-perovskite type ferromagnetic nitrides are also good candidates for application to spintronics. For instance, large negative P is also predicted in Fe_4B and Fe_4C,[11] and the perpendicular magnetic anisotropy is observed in Mn_4N films.[12,13] Systematic analyses of magnetic moments in $Co_xFe_{4-x}N$ ($x = 0$, 3, 4) help us to understand features of these anti-perovskite type ferromagnetic nitrides.

II. EXPERIMENTAL METHOD

XMCD measurements were performed for epitaxially grown Au(3 nm)/Fe_4N(10 nm)/$LaAlO_3$(001) (sample A), Au (3 nm)/Co_4N(10 nm)/STO(001) (sample B), and CaF_2(2 nm)/Co_3FeN(10 nm)/STO(001) (sample C) at the undulator beamline BL23SU[14] of SPring-8 in Japan. We measured x-ray absorption spectra (XAS) and XMCD spectra at Fe and Co $L_{2,3}$-edges using the total electron yield method, and deduced

a)Author to whom correspondence should be addressed. Electronic mail: suemasu@bk.tsukuba.ac.jp.

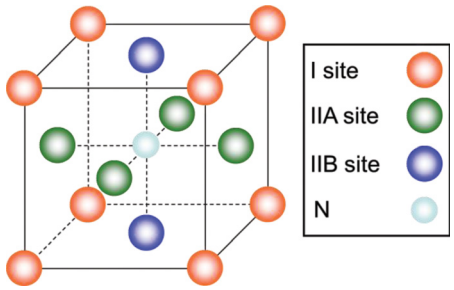

FIG. 1. Lattice structure of anti-perovskite type 3*d* transition metal nitrides.

site-averaged m_{orb} and m_{spin} per Fe and Co atoms in $Co_xFe_{4-x}N$ films. Circularly polarized x-rays were incident perpendicular to the film surface at 300 K. External magnetic fields of ±3 T were applied to perpendicular to the sample surface during measurements, and we used their averaged spectra for analysis of magnetic moments to ensure the accuracy of the measurement. 3 T was enough to saturate the magnetization of the samples.

III. RESULTS AND DISCUSSION

Figures 2(a) and 2(b) show the XAS and XMCD spectra at Fe $L_{2,3}$-edges of samples A and C, respectively, measured at 300 K. Figures 3(a) and 3(b) show those at Co $L_{2,3}$-edges for samples B and C, respectively. Clear XMCD spectra were observed at $L_{2,3}$-edges in all the samples. We can observe the satellite peaks by approximately 2−3 eV higher than the main peaks of $L_{2,3}$-edges, as indicated by arrows in Figs. 2 and 3. We considered that these satellite peaks, which are also observed in the reported XAS spectra of Fe_4N films,[15,16] were attributed to intrinsic electronic structures of anti-perovskite nitrides. Details will be presented elsewhere. The structure of F *K*-edge in Fig. 2(b) is attributed to the CaF_2 capping layer. The sign of XMCD signal at Fe $L_{2,3}$-edges in sample C was the same as that at Co $L_{2,3}$-edges, meaning that ferromagnetic order is created

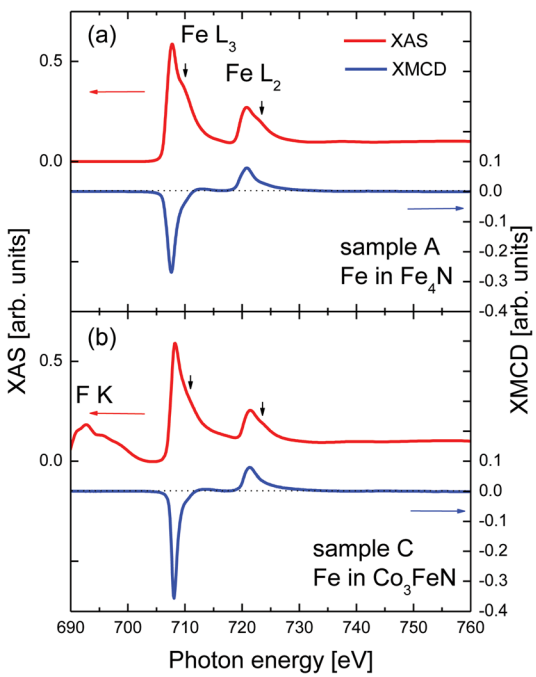

FIG. 2. XAS and XMCD spectra at Fe $L_{2,3}$-edges of (a) Fe_4N (sample A) and (b) Co_3FeN (sample C) observed at 300 K.

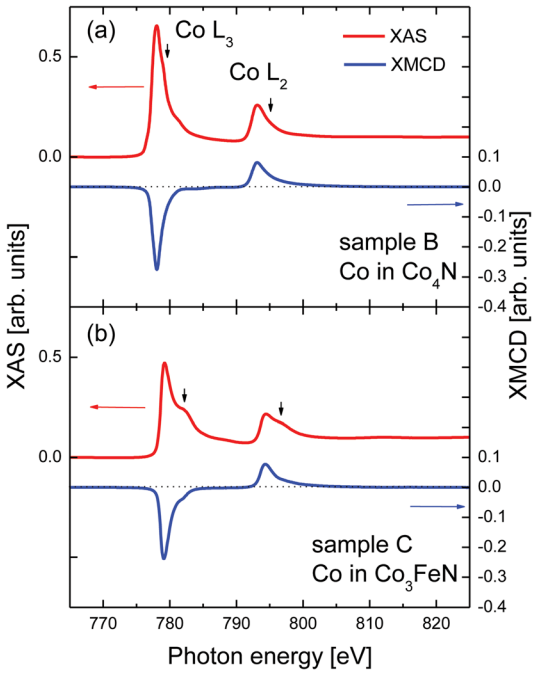

FIG. 3. XAS and XMCD spectra at Co $L_{2,3}$-edges of (a) Co_4N (sample B) and (b) Co_3FeN (sample C) observed at 300 K.

between the Fe and Co atoms in sample C. We evaluated the site-averaged m_{orb} and m_{spin} per Fe and Co atoms of this sample by applying magneto-optical sum-rules analysis.[17–19] The backgrounds of the XAS spectra were removed by subtracting the two-step function from the raw XAS spectra. The electron hole numbers of 3*d* orbital (N_h) of Fe and Co in samples A-C were determined to be 4.36 ± 0.16 (Fe in Fe_4N), 2.71 ± 0.41 (Co in Co_4N), 4.31 ± 0.70 (Fe in Co_3FeN), and 2.43 ± 0.29 (Co in Co_3FeN), respectively, using the XAS spectra of the samples, the standard XAS spectra of bcc-Fe and hcp-Co, and N_h values in bcc-Fe (3.39) and hcp-Co (2.49).[17,20] The site-averaged m_{orb} and m_{spin} of the samples are summarized in Table I. The theoretically calculated values of m_{spin} for Fe_4N and Co_4N are also shown for comparison.[20,21] Corrected site-averaged m_{orb} and m_{spin} values by taking the saturation effect[22] are listed in parentheses in Table I. We used the correction factors in case that the light is incident normal to the film plane with the 10-nm-thick Fe and Co films, shown in Ref. 22. The m_{orb} values of Fe atoms were close to those of Co atoms. The m_{spin} values per atoms were evaluated to be approximately 1.87 (Fe in Fe_4N), 1.43 (Co in Co_4N), 1.91 (Fe in Co_3FeN), and 1.47 μ_B (Co in Co_3FeN), respectively. Deduced m_{spin} values of samples A and B were smaller than those calculated values by first-principle calculations. This underestimation might come from using the correction factors for pure Fe and Co instead of those for Fe_4N and Co_4N. According to Ref. 23, the band hybridization between 3*d* orbit of II site atoms and 2*p* orbit of nitrogen atoms induces the large m_{spin} at I sites, but suppresses that of II sites.[23] Obtained site-averaged m_{spin} values of Fe and Co atoms in sample C are almost the same as those of samples A and B, respectively. This implies that Fe and Co atoms in sample C were located both at I and II sites, similar to Fe_4N and Co_4N. Further structural analysis is required in order to reveal the location of Fe and Co atoms in Co_3FeN unit cell.

TABLE I. Orbital and spin magnetic moments of Fe and Co atoms in Fe_4N, Co_4N, and Co_3FeN deduced by XMCD and theoretical calculations. Corrected moment values of samples after taking the saturation effect into account are listed in parentheses.

		Magnetic moment [μ_B per atom]			
Compounds	Atoms	m_{orb}	m_{spin}	Method	Reference
Fe_4N	Fe(300 K)	0.10 ± 0.01	1.72 ± 0.05	XMCD	This work
	(Corrected)	(∼0.19)	(∼1.87)		
	Fe(0 K)	…	2.29	Calculation	20
Co_4N	Co(300 K)	0.10 ± 0.01	1.31 ± 0.15	XMCD	This work
	(Corrected)	(∼0.14)	(∼1.43)		
	Co(0 K)	…	1.61	Calculation	21
Co_3FeN	Fe(300 K)	0.08 ± 0.01	1.76 ± 0.19	XMCD	This work
	(Corrected)	(∼0.16)	(∼1.91)		
	Co(300 K)	0.11 ± 0.01	1.33 ± 0.12	XMCD	This work
	(Corrected)	(∼0.15)	(∼1.47)		

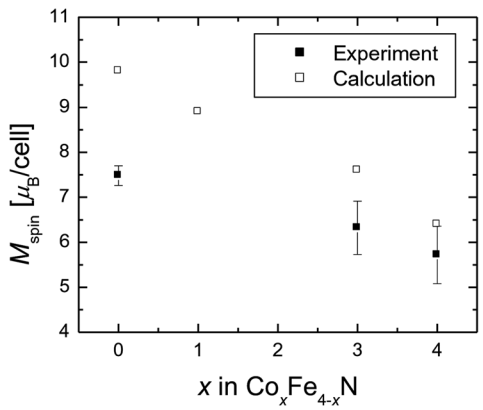

FIG. 4. Relationship between M_{spin} and x values in $Co_xFe_{4-x}N$ films.

Figure 4 displays the relationship between spin magnetic moments per unit cell (M_{spin}) in $Co_xFe_{4-x}N$ and x values (Co/Fe ratio). M_{spin} values deduced from the XMCD measurements (■) were 7.48 (Fe_4N), 6.32 (Co_3FeN), and 5.72 μ_B (Co_4N), respectively. These values are a little smaller than those calculated by first-principle calculations (□).[3] M_{spin} was decreased linearly with x in $Co_xFe_{4-x}N$. This behavior is in good agreement with the theory presented in Ref. 3.

IV. SUMMARY

Site-averaged m_{orb} and m_{spin} of Fe and Co atoms in MBE-grown epitaxial $Co_xFe_{4-x}N$ ($x = 0, 3, 4$) films were evaluated using XMCD measurements. Site-averaged m_{spin} values of Co_3FeN were deduced to be 1.91 μ_B per Fe atom and 1.47 μ_B per Co atom at 300 K. These values are almost the same as those of Fe_4N and Co_4N, respectively. These results imply that Fe and Co atoms in the Co_3FeN film are randomly located both at I and II sites. M_{spin} values of $Co_xFe_{4-x}N$ films were decreased linearly with increasing x. This trend was well explained by the first-principle calculation.

ACKNOWLEDGMENTS

XMCD measurements were performed at SPring-8 BL23SU under Nanonet Support Proposals (Proposal Nos. 2010B3876, 2011A3872, and 2012B3840). The authors thank Professor T. Oguchi of Osaka University for private discussions. K. Ito and T. Suemasu also thank Dr. N. Ota and Professor K. Asakawa of the Tsukuba Nano-Tech Human Resource Development Program at the University of Tsukuba for useful discussions.

[1]S. Kokado, N. Fujima, K. Harigaya, H. Shimizu, and A. Sakuma, Phys. Rev. B **73**, 172410 (2006).
[2]Y. Imai, Y. Takahashi, and T. Kumagai, J. Magn. Magn. Mater. **322**, 2665 (2010).
[3]Y. Takahashi, Y. Imai, and T. Kumagai, J. Magn. Magn. Mater. **323**, 2941 (2011).
[4]A. Narahara, K. Ito, T. Suemasu, Y. K. Takahashi, A. Rajanikanth, and K. Hono, Appl. Phys. Lett. **94**, 202502 (2009).
[5]Y. Komasaki, M. Tsunoda, S. Isogami, and M. Takahashi, J. Appl. Phys. **105**, 07C928 (2009).
[6]K. Ito, G. H. Lee, H. Akinaga, and T. Suemasu, J. Cryst. Growth **322**, 63 (2011).
[7]K. Ito, K. Harada, K. Toko, H. Akinaga, and T. Suemasu, J. Cryst. Growth **336**, 40 (2011).
[8]T. Sanai, K. Ito, K. Toko, and T. Suemasu, J. Cryst. Growth **357**, 53 (2012).
[9]K. Ito, G. H. Lee, K. Harada, M. Suzuno, T. Suemasu, Y. Takeda, Y. Saitoh, M. Ye, A. Kimura, and H. Akinaga, Appl. Phys. Lett. **98**, 102507 (2011).
[10]K. Ito, K. Harada, K. Toko, M. Ye, A. Kimura, Y. Takeda, Y. Saitoh, H. Akinaga, and T. Suemasu, Appl. Phys. Lett. **99**, 252501 (2011).
[11]Z. Q. Lv, Y. Gao, S. H. Sun, M. G. Qv, Z. H. Wang, Z. P. Shi, and W. T. Fu, J. Magn. Magn. Mater. **333**, 39 (2013).
[12]K. M. Ching, W. D. Chang, T. S. Chin, J. G. Duh, and H. C. Ku, J. Appl. Phys. **76**, 6582 (1994).
[13]M. Tsunoda and K. Kabara, *presented at the International Conference of the Asian Union of Magnetics Societies (ICAUMS)* (2012), 2pPS–47.
[14]Y. Saitoh, Y. Fukuda, Y. Takeda, H. Yamagami, S. Takahashi, Y. Asano, T. Hara, K. Shirasawa, M. Takeuchi, T. Tanaka, and H. Kitamura, J. Synchrotron Radiat. **19**, 388 (2012).
[15]C. Sánchez-Hanke, R. Gonzalez-Arrabal, J. E. Prieto, E. Andrzejewska, N. Gordillo, D. O. Boerma, R. Loloee, J. Skuza, and R. A. Lukaszew, J. Appl. Phys. **99**, 08B709 (2006).
[16]Y. Takagi, K. Isami, I. Yamamoto, T. Nakagawa, and T. Yokoyama, Phys. Rev. B **81**, 035422 (2010).
[17]B. T. Thole, P. Carra, F. Sette, and G. van der Laan, Phys. Rev. Lett. **68**, 1943 (1992).
[18]P. Carra, B. T. Thole, M. Altarelli, and X. D. Wang, Phys. Rev. Lett. **70**, 694 (1993).
[19]C. T. Chen, Y. U. Idzerda, H. J. Lin, N. V. Smith, G. Meigs, E. Chaban, G. H. Ho, E. Pellegrin, and F. Sette, Phys. Rev. Lett. **75**, 152 (1995).
[20]A. Sakuma, J. Magn. Magn. Mater. **102**, 127 (1991).
[21]S. F. Matar, A. Houari, and M. A. Belkhir, Phys. Rev. B **75**, 245109 (2007).
[22]R. Nakajima, J. Stöhr, and Y. U. Idzerda, Phys. Rev. B **59**, 6421 (1999).
[23]X. G. Ma, J. J. Jiang, P. Liang, J. Wang, Q. Ma, and Q. K. Zhang, J. Alloys Compd. **480**, 475 (2009).